

On the Impact of $f(Q)$ Gravity on the Large Scale Structure

Simran Arora

Birla Institute of Technology & Science-Pilani,
Hyderabad Campus, India

Collaboration with: Oleksii Sokoliuk, Subhrat Praharaj, Alexander Baransky, P.K. Sahoo
[arxiv: 2303.17341 \(MNRAS, 2023\)](#)

Gravity and Cosmology 2024, Yukawa Institute for Theoretical Physics, Kyoto University

- Foundations of General Relativity and going beyond GR
- Modified gravity theories
- Constructed $f(Q)$ model in our work

- Successes of Λ CDM:
 - ▶ Primarily consistent with observations,
 - ▶ Describe the evolution and formation of structures,
 - ▶ Primordial nucleosynthesis,
 - ▶ Dark energy and dark matter scenario.

¹A. Joyce et al., *Phys. Rept.* **568**, 1-98 (2015).

²S. Tsujikawa. Introductory review of cosmic inflation. In 2nd Tah Poe School on Cosmology: Modern Cosmology, 4 (2003).

³E. Di Valentino et al., *Astropart. Phys.* **131**, 102605 (2021).

⁴E. Di Valentino et al., *Astropart. Phys.* **131**,102604 (2021).

- Successes of Λ CDM:
 - ▶ Primarily consistent with observations,
 - ▶ Describe the evolution and formation of structures,
 - ▶ Primordial nucleosynthesis,
 - ▶ Dark energy and dark matter scenario.
- Theoretical issues with Λ CDM:
 - ▶ Cosmological constant problem: Discrepancy between the theoretical and observed values of the cosmological constant¹, (Order of 10^{120})
 - ▶ Fine-tuning of cosmological parameters², (Why is it so fine-tuned?)
 - ▶ H_0 tension³,
 - ▶ S_8 tension⁴.

¹A. Joyce et al., *Phys. Rept.* **568**, 1-98 (2015).

²S. Tsujikawa. Introductory review of cosmic inflation. In 2nd Tah Poe School on Cosmology: Modern Cosmology, 4 (2003).

³E. Di Valentino et al., *Astropart. Phys.* **131**, 102605 (2021).

⁴E. Di Valentino et al., *Astropart. Phys.* **131**,102604 (2021).

- Successes of Λ CDM:
 - ▶ Primarily consistent with observations,
 - ▶ Describe the evolution and formation of structures,
 - ▶ Primordial nucleosynthesis,
 - ▶ Dark energy and dark matter scenario.
- Theoretical issues with Λ CDM:
 - ▶ Cosmological constant problem: Discrepancy between the theoretical and observed values of the cosmological constant¹, (Order of 10^{120})
 - ▶ Fine-tuning of cosmological parameters², (Why is it so fine-tuned?)
 - ▶ H_0 tension³,
 - ▶ S_8 tension⁴.
- Alternatives of Λ CDM:
 - ▶ Early dark energy
 - ▶ Dynamical dark energy
 - ▶ Interacting dark matter and dark energy
 - ▶ Modified gravity models

¹ A. Joyce et al., *Phys. Rept.* **568**, 1-98 (2015).

² S. Tsujikawa. Introductory review of cosmic inflation. In 2nd Tah Poe School on Cosmology: Modern Cosmology, 4 (2003).

³ E. Di Valentino et al., *Astropart. Phys.* **131**, 102605 (2021).

⁴ E. Di Valentino et al., *Astropart. Phys.* **131**,102604 (2021).

The standard formulation of GR is based on various assumptions:

- 4-dimensional Lorentzian manifold
- metric structure g
- connection Γ , or a covariant derivative ∇
- derivative is metric compatibility $\nabla_\alpha g_{\mu\nu} = 0$
- derivative is torsion-free, i.e. $(\nabla_\mu \nabla_\nu - \nabla_\nu \nabla_\mu) f = T_{\mu\nu}^\gamma \partial_\gamma f = 0$
- action linear in curvature (famous Einstein-Hilbert action)

The standard formulation of GR is based on various assumptions:

- 4-dimensional Lorentzian manifold
- metric structure g
- connection Γ , or a covariant derivative ∇
- derivative is metric compatibility $\nabla_{\alpha} g_{\mu\nu} = 0$
- derivative is torsion-free, i.e. $(\nabla_{\mu} \nabla_{\nu} - \nabla_{\nu} \nabla_{\mu}) f = T_{\mu\nu}^{\gamma} \partial_{\gamma} f = 0$
- action linear in curvature (famous Einstein-Hilbert action)

Let us think about these assumptions more!

- 4-dimensions \rightarrow why not more?
 - ▶ Kaluza-Klein theories, Rep. Prog. Phys. 50 1087 (1987) - One extra dimension
 - ▶ Bosonic string theory - 26 dimensions
 - ▶ Superstring theory - 10 dimensions
- Connection: Why $\nabla_{\alpha} g_{\mu\nu} = 0$, $T_{\mu\nu}^{\gamma} = 0$?
 - ▶ Einstein-Cartan theory in 1920s
 - ▶ Teleparallel equivalent to GR in the late 1920s
 - ▶ Pelegrini, Hayashi, Nakano: New Teleparallel gravity in the 1960s and 1970s ($\nabla_{\alpha} g_{\mu\nu} = 0$)
 - ▶ Metric affine theory in the late 1970s ($\nabla_{\alpha} g_{\mu\nu} \neq 0$ and $T_{\mu\nu}^{\gamma} \neq 0$)

- We know the Einstein-Hilbert action $S = \frac{1}{2k} \int R \sqrt{-g} d^4x$.
In 1970s, Budchal introduces non-linear lagrangians
In the 1980s, Starobinsky worked on inflationary models
In the late 1990s, dark energy models came into picture
In the early 2000s, Modified theories of gravity such as $f(R)$ gravity⁵, 2007 $f(T)$ gravity⁶,
2015 $f(T, B)$ gravity, 2017 $f(Q)$ gravity⁷
- From then onwards, plenty of theories are coming into the picture!

⁵S. D. Odintsov, V. K. Oikonomou, *Phys. Rev. D* **99**, 064049 (2019); V. K. Oikonomou, *Phys. Rev. D* **103**, 044036 (2021).

⁶Yi-Fu Cai et al., *Rep. Prog. Phys.* **79**, 106901 (2016); R. C. Nunes, *J. Cosmol. Astropart. Phys.* **05**, 052 (2018).

⁷R. Lazkoz et al., *Phys. Rev. D* **100**, 104027 (2019).

Modified Gravity Theories



Figure 1: arxiv: 2105.12582

Geometrical Representation

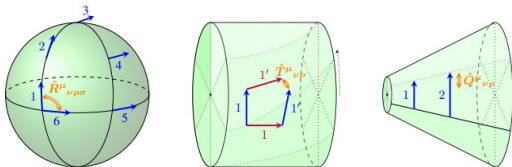


Figure 2: Schematic geometrical representation of the curvature, torsion, and non-metricity tensors by their effect on the parallel transport of vectors.

- **Curvature:** It could be deduced that in a non-Euclidean space, when a tensor is parallelly shifted along a closed curve till returning to the initial point, the resultant vector may not necessarily be the same as the original vector.

$$R^{\mu}_{\nu\sigma\lambda} = \partial_{\sigma}\Gamma^{\mu}_{\lambda\nu} - \partial_{\lambda}\Gamma^{\mu}_{\sigma\nu} + \Gamma^{\mu}_{\sigma\delta}\Gamma^{\delta}_{\lambda\nu} - \Gamma^{\mu}_{\lambda\delta}\Gamma^{\delta}_{\sigma\nu}.$$

- **Torsion:** The presence of torsion cracks parallelograms into pentagons.

$$T^{\alpha}_{\mu\nu} = \Gamma^{\alpha}_{\mu\nu} - \Gamma^{\alpha}_{\nu\mu}.$$

- **Non-metricity:** The length of a vector changes when being transported in parallel in a space with non-metricity.

$$Q_{\alpha\mu\nu} = \nabla_{\alpha}g_{\mu\nu}.$$

The starting point of these theories is again the Einstein-Hilbert action-like action⁸

$$S_{metric\ affine} = \frac{1}{2k} \int \bar{R} \sqrt{-g} d^4x, \quad (1)$$

where $\bar{R} = \underbrace{G + B}_{GR} + \underbrace{T - B_T}_{TEGR} + \underbrace{Q + B_Q}_{STEGR} + C$.

- Ricci scalar $R = G + B$, which is used in GR, where $G = g^{\mu\nu} (\Gamma_{\mu\sigma}^{\alpha} \Gamma_{\alpha\nu}^{\sigma} - \Gamma_{\mu\nu}^{\sigma} \Gamma_{\alpha\sigma}^{\alpha})$,
- Torsion scalar TEGR T ,
- Non-metricity scalar used in STEGR Q ,
- C is torsion-non-metricity cross terms
- B_T, B_Q are torsional and non-metricity boundary terms

Note: When torsion and nonmetricity are assumed to vanish, one works in the standard GR (LHS would not be zero but equal to the Ricci scalar).

Assuming that nonmetricity vanishes gives TEGR, whereas the vanishing of torsion gives STEGR. Cross-term C vanishes when either torsion or nonmetricity vanishes.

⁸<https://doi.org/10.1103/PhysRevD.104.024010>

- The strategy is: We work in a generic metric-affine geometry (M, g, Γ) and we compute the covariant derivative of the metric, perform cyclic permutations of the indices and finally isolate the connection coefficients $\Gamma_{\mu\nu}^{\alpha}$. This finally allows us to solve for the connection

$$\Gamma_{\mu\nu}^{\alpha} = \left\{ \begin{array}{c} \alpha \\ \mu\nu \end{array} \right\} + K_{\mu\nu}^{\alpha} + L_{\mu\nu}^{\alpha}, \quad (2)$$

where $K_{\mu\nu}^{\alpha} = \frac{1}{2} T_{\mu\nu}^{\alpha} + T_{(\mu}^{\alpha}{}_{\nu)}$ and $L_{\mu\nu}^{\alpha} = \frac{1}{2} Q_{\mu\nu}^{\alpha} + Q_{(\mu}^{\alpha}{}_{\nu)}$ are contorsion and disformation tensors. A flat, torsionless connection can be written as

$$\Gamma_{\mu\nu}^{\alpha} = \frac{\partial x^{\alpha}}{\partial \xi^{\beta}} \partial_{\mu} \partial_{\nu} \xi^{\beta} \quad (3)$$

They can be set to zero globally by an appropriate choice of coordinates. This is known as the coincident gauge. The Symmetric Teleparallel Equivalent of GR gravity is described by the action

$$S = -\frac{1}{2k} \int Q(g, \xi) \sqrt{-g} d^4x + S_{matter}. \quad (4)$$

This opens the door for yet another generalization of the geometrical trinity of gravity.

$$S = -\frac{1}{2k} \int f(Q) \sqrt{-g} d^4x + S_{matter}. \quad (5)$$

The motivation for this non-linear extension is that the added freedom in choosing a function f may help in explaining the accelerated expansion of the universe, structure formation, and other phenomena which in the trinity of GR requires the introduction of dark energy and dark matter.

Overview of $f(Q)$ gravity

The action for $f(Q)$ gravity is defined as⁹

$$S = -\frac{1}{2\kappa} \int f(Q) \sqrt{-g} d^4x + \int L_m \sqrt{-g} d^4x.$$

$$Q_{\alpha\mu\nu} = \nabla_\alpha g_{\mu\nu}, \quad Q = -Q_{\alpha\mu\nu} P^{\alpha\mu\nu}, \quad Q_\alpha = g^{\mu\nu} Q_{\alpha\mu\nu}, \quad \tilde{Q}_\alpha = g^{\mu\nu} Q_{\mu\alpha\nu}$$
$$P^\alpha_{\mu\nu} = -\frac{1}{2} L^\alpha_{\mu\nu} + \left(Q^\alpha - \tilde{Q}^\alpha \right) \frac{g_{\mu\nu}}{4} - \frac{1}{4} \delta^\mu_{(\nu} Q_{\nu)}, \quad L^\alpha_{\mu\nu} = \frac{1}{2} \left(Q^\alpha_{\mu\nu} - Q_{(\mu\nu)\alpha} \right)$$

The metric and connection field equations are

$$\frac{2}{\sqrt{-g}} \nabla_\alpha (\sqrt{-g} f_Q P^\alpha_{\mu\nu}) + \frac{1}{2} g_{\mu\nu} f + f_Q \left(P_{\mu\alpha\beta} Q_\nu^{\alpha\beta} - 2 Q_{\alpha\beta\mu} P^{\alpha\beta}_\nu \right) = 8\pi G \mathcal{T}_{\mu\nu}, \quad (6)$$

$$\nabla_\mu \nabla_\nu (\sqrt{-g} f_Q P^{\mu\nu}_\alpha) = 0. \quad (7)$$

where $f_Q = \frac{df}{dQ}$.

⁹J. B. Jimenez, L. Heisenberg, T. Kovisto, *Phys. Rev. D* **98**, 044048 (2018).

Cosmology in $f(Q)$

For FLRW spacetime, the non-metricity scalar is $Q = 6H^2$ and resulting cosmological equations are

$$3H^2 = \frac{\kappa}{2f_Q} \left(\rho_m + \frac{f}{2} \right),$$
$$(12H^2 f_{QQ} + f_Q) \dot{H} = -\frac{\kappa}{2} (\rho_m + p_m).$$

Here, we use¹⁰

$$f(Q) = Q + \alpha Q_0 \left(1 - e^{-\beta \sqrt{Q/Q_0}} \right), \quad Q_0 = 6H_0^2$$
$$\alpha = -\frac{e^\beta (-1 + \Omega_{m0})}{-1 + e^\beta - \beta}, \quad (\text{using first Friedmann equation}) \quad (8)$$

In order to solve the field equations for the Hubble parameter, we use¹¹

$$\dot{H} = aH \frac{dH}{da}, \quad \dot{H}|_{z=0} = -H_0^2 (1 + q_0). \quad (9)$$

¹⁰T. Harko et al., *Phys. Rev. D* **98**, 084043 (2018); K. F. Anagnostopoulos et al., *Eur. Phys. J. C* **83**, 58 (2023); W. Khyllep et al., *Phys. Rev. D* **107**, 044022 (2023).

¹¹M. J. Reid, D. W. Pesce, A. G. Riess, *Astrophys. J. Lett.* **886**, L27 (2019); N. Aghanim et al., *Astron. Astrophys.* **641**, A6 (2020).

- Hubble data: Points from cosmic chronometers ¹²
- SNela (Pantheon) samples: Discovered from the Pan-STARRS1 (PS1) Medium Deep Survey, Low z, SNLS, SDSS, and HST ¹³
- BAO dataset ¹⁴

Table 1: Best-fit values of model parameters and statistical analysis

Datasets	H_0	Ω_{m0}	β
Hubble (OHD)	66.9 ± 3.3	$0.320^{+0.055}_{-0.070}$	4.3 ± 1.9
OHD+SNela	68.9 ± 1.7	$0.290^{+0.028}_{-0.020}$	$5.3^{+1.8}_{-1.0}$
OHD+SNela+BAO	68.9 ± 1.6	0.292 ± 0.016	5.6 ± 1.25

¹²G. S. Sharov, V. O. Vasiliev, *Mathematical Modelling and Geometry* **6**, 1 (2018).

¹³D. M. Scolnic et al., *Astrophys. J.* **859**, 101 (2018).

¹⁴P. A. R. Ade et al., *Astron. Astrophys.* **594**, A13 (2015); S. Basilakos, A. Pouri, *Mon. Not. R. Astron. Soc.* **423**, 3761, (2012); D. J. Eisenstein et al., *Astrophys. J.* **633**, 560 (2005).

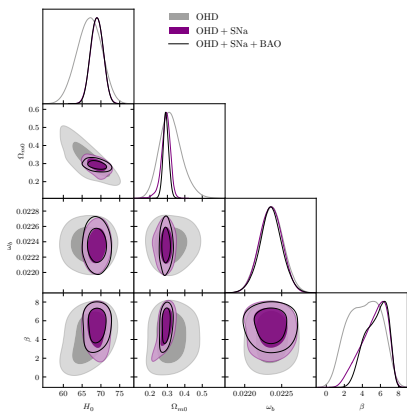


Figure 3: MCMC best fits from $H(z)$ (OHD), Pantheon, and BAO datasets and joint distribution.

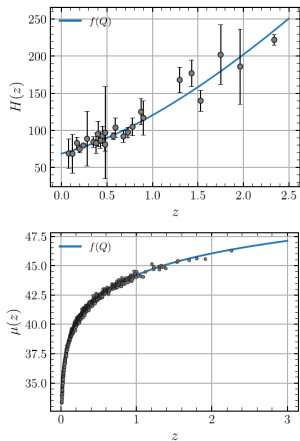


Figure 4: Evolution of the Hubble parameter and distance modulus.

Cosmological Parameters

$$q = -1 - \frac{\dot{H}}{H^2}, \quad r = \frac{\ddot{a}}{aH^3}, \quad s = \frac{r-1}{3(q-1/2)}. \quad (10)$$

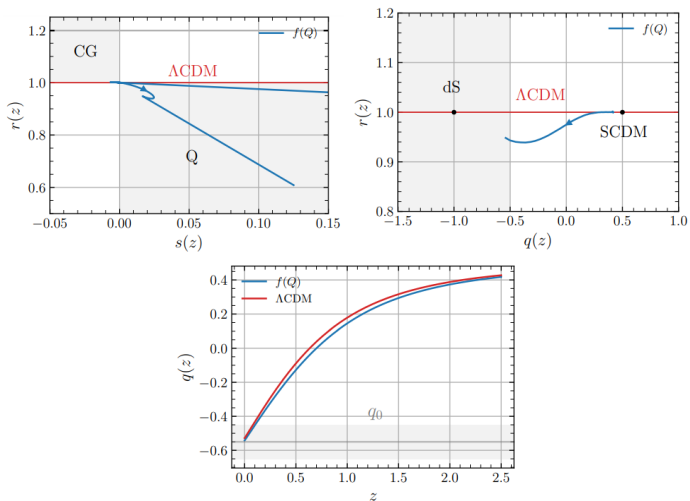


Figure 5: Evolution of statefinder pairs and deceleration parameter.

Let us consider the perturbed line element in Newtonian gauge

$$ds^2 = -(1 + 2\Psi)dt^2 + a^2(1 - 2\Phi)\delta_{ij}dx^i dx^j, \quad (11)$$

where Φ and Ψ are the two gravitational potentials. For MG theories, a model-independent framework is usually adopted to relate the gravitational potentials to the linear matter density perturbations $\delta\rho_m$.

Furthermore, assuming the quasistatic approximation, it can be shown that for $f(Q)$ gravity, the two gravitational potentials coincide, $\Phi = \Psi$, as in GR. However, the Poisson equation, which defines the relation between the linear matter perturbations, $\delta\rho_m$, and the gravitational potentials in Fourier space, reads

$$-k^2\Psi = 4\pi\frac{G_N}{f_Q}a^2\rho_m\delta_m. \quad (12)$$

where $\delta_m = \delta\rho_m/\rho_m$ is the density contrast. We thus end up with the simple evolution equation for the overdensity¹⁵,

$$\delta_m'' + 2H\delta_m' = \frac{4\pi G_N}{f_Q}\rho_m\delta_m. \quad (13)$$

which governs the growth of structures in the quasistatic limit.

¹⁵ J. B. Jimenez, L. Heisenberg, T. Koivisto, S. Pekar, *Phys. Rev. D*, **101**, 103507 (2020)

N-body Simulations

- We perform N-body simulations of the comoving box that contains DM+baryonic matter and dark energy in exponential $f(Q)$ gravitation and compare our results with the large-scale structure of concordance Λ CDM cosmology.
- For that aim, we will use the publicly available code ME-GADGET ([Galaxies with Dark matter and Gas Interact](#)), a modification of the well-known hydrodynamical N-body code GADGET2. It has been modified for generality to perform simulations for practically any cosmological model. The code above is described in the pioneering works of¹⁶, whereas the tests are provided in¹⁷.
- This code as an input needs tables with Hubble flow H/H_0 and the deviation of effective gravitational constant from the Newtonian one G_{eff}/G_N . One can find the effective gravitational constant exact form in¹⁸ as

$$G_{\text{eff}} = \frac{G_N}{f_Q}. \quad (14)$$

¹⁶ R. An et al., *Mon. Not. R. Astron. Soc.* **489**, 297 (2019); J. Zhang et al., *Astrophys. J. Lett.* **875**, L11 (2019).

¹⁷ J. Zhang et al., *Phys. Rev. D* **98**, 103530 (2018).

¹⁸ J. B. Jimenez et al., *Phys. Rev. D* **101**, 103507 (2020).

- One needs to define various parameters to produce the simulations. We assume the particle number to be $N = 512^3$. The simulation box has periodic vacuum boundary conditions and sides with length 10 Mpc/h. Initial conditions were produced with the `Simp2LPTic` code¹⁹, and glass files (pre-initial conditions) were generated with the use of `ccvt-preic`²⁰. The capacity-constrained Voronoi tessellation (`ccvt`) method is an alternative method to produce a uniform and isotropic particle distribution to generate pre-initial conditions.
- Moreover, cosmological parameters were borrowed from our MCMC constraints, discussed earlier:
 - ▶ $h = H_0/100 = 0.689 \pm 0.016$,
 - ▶ $\Omega_{\Lambda 0} = 0.708$,
 - ▶ $\Omega_{m0} = 0.292 \pm 0.016$,
 - ▶ $\Omega_b = 0.0493$.
- Moreover, matter power spectrum amplitude is assumed to be $\sigma_8 = 0.811 \pm 0.006$ and the spectrum index of scalar perturbations as $n_s = 0.9649 \pm 0.0042$ ²¹ (power spectrum were constructed using code `CAMB`, see²²).

¹⁹ (see GitHub repository <https://github.com/liambx/Simp2LPTic>)

²⁰ (check <https://github.com/liaoshong/ccvt-preic>)

²¹ Y. Akrami et al., *Astron. Astrophys.* **641**, A10 (2020).

²² A. Lewis, A. Challinor, *Astrophysics Source Code Library*, record ascl:1102.026, (2011).

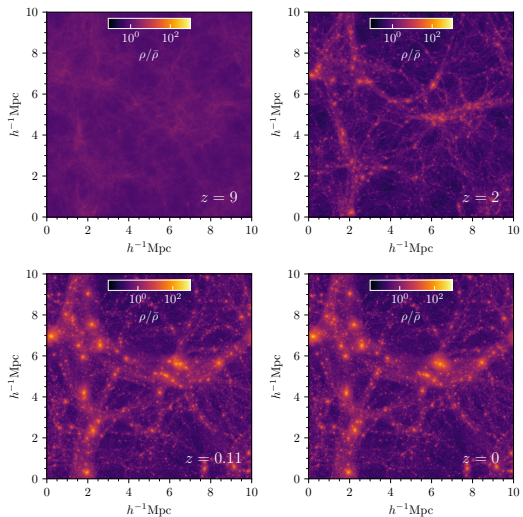
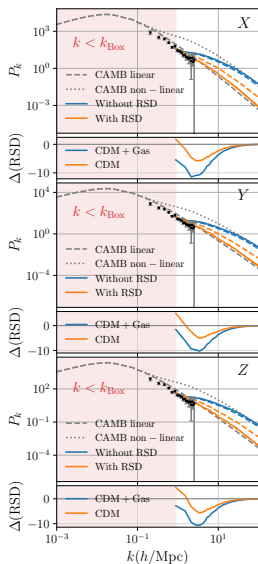
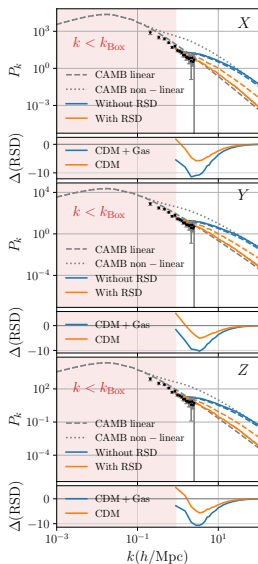


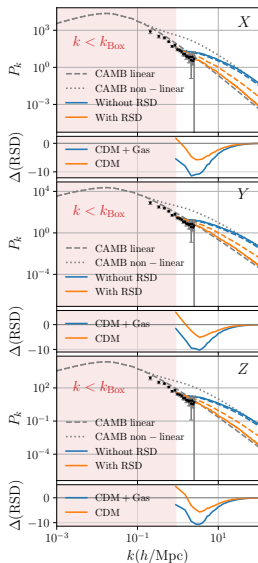
Figure 6: N-body simulations snapshot of overdensity on different redshifts.



- Matter power spectrum with/without RSDs for $f(Q)$ gravity vs. CAMB linear/non-linear $P(k)$ for Λ CDM. Dashed N-body $P(k)$ represents the CDM-only power spectrum, while the solid line represents CDM+Gas $P(k)$. Error bars represent Ly- α forest observations on high z .

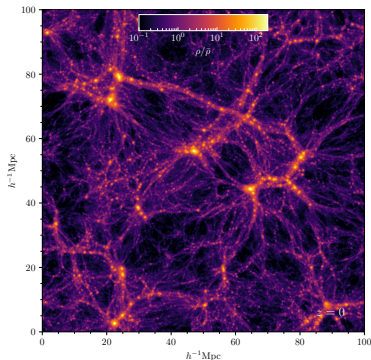


- Matter power spectrum with/without RSDs for $f(Q)$ gravity vs. CAMB linear/non-linear $P(k)$ for Λ CDM. Dashed N-body $P(k)$ represents the CDM-only power spectrum, while the solid line represents CDM+Gas $P(k)$. Error bars represent Ly- α forest observations on high z .
- We consequently compare the matter power spectrum with/without RSDs directed along both X, Y, and Z axes. As we noticed during numerical analysis, up to some k near k_{Box} limit for our simulation, $P(k)$ spectrum in Fourier space does reconstruct non-linear matter power spectrum, given by CAMB, while Redshift-Space Distorted (RSD) one behaves like the linear matter power spectrum, as expected.

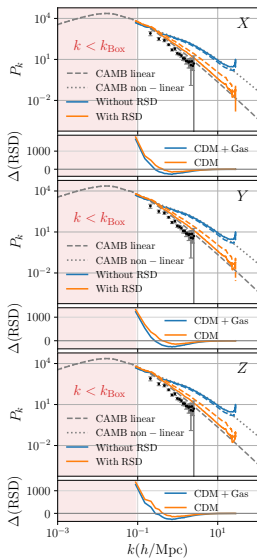


- Matter power spectrum with/without RSDs for $f(Q)$ gravity vs. CAMB linear/non-linear $P(k)$ for Λ CDM. Dashed N-body $P(k)$ represents the CDM-only power spectrum, while the solid line represents CDM+Gas $P(k)$. Error bars represent Ly- α forest observations on high z .
- We consequently compare the matter power spectrum with/without RSDs directed along both X, Y, and Z axes. As we noticed during numerical analysis, up to some k near k_{Box} limit for our simulation, $P(k)$ spectrum in Fourier space does reconstruct non-linear matter power spectrum, given by CAMB, while Redshift-Space Distorted (RSD) one behaves like the linear matter power spectrum, as expected.
- Also, it is worth noticing that the difference between RSD and regular matter power spectrum is bigger for the CDM+Gas case. Finally, the effect of RSDs in our simulations is almost isotropic, so that $\Delta(\text{RSD})$ differs only by a few per cent with the change of RSD direction axis.

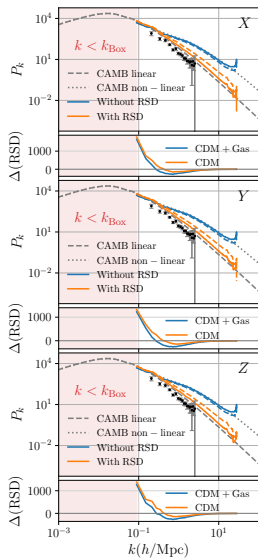
Large L_{Box}



- This is an analysis of N-body simulation for a bigger simulation box size, namely with $L_{\text{box}} = 100h^{-1}\text{Mpc}$. In that case, we only differ in force resolution, while other cosmological parameters are assumed to be the same. At first, we, as usual, plot the CDM overdensity field for vanishing redshift.
- As an obvious consequence of a larger box size, one can notice that maximum wavenumber k grew to $k_{\text{max}} \approx 20 h/\text{Mpc}$.



- Matter power spectrum with/without RSDs for $f(Q)$ gravity vs. CAMB linear/non-linear $P(k)$ for Λ CDM. Dashed N-body $P(k)$ represents the CDM-only power spectrum, while the solid line represents CDM+Gas $P(k)$. Error bars represent Ly- α forest observations on high z . For this case, we have assumed a large simulation box size of $100h^{-1}\text{Mpc}$.



- Matter power spectrum with/without RSDs for $f(Q)$ gravity vs. CAMB linear/non-linear $P(k)$ for Λ CDM. Dashed N-body $P(k)$ represents the CDM-only power spectrum, while the solid line represents CDM+Gas $P(k)$. Error bars represent Ly- α forest observations on high z . For this case, we have assumed a large simulation box size of $100h^{-1}\text{Mpc}$.
- Even at such big scales, our matter power spectrum, derived from the corresponding N-body simulation, converges with the theoretical prediction from CAMB code with up to sub-percent accuracy. As we noticed previously for the small simulation box, the axis of redshift-space distortions had a very small impact on the matter power spectrum. This statement also holds for large L_{box} .

- We first performed MCMC analysis for our $f(Q)$ model to obtain best-fit values of free parameters. To test the fits provided by MCMC, we obtained theoretical predictions for the Hubble parameter $H(z)$, deceleration parameter $q(z)$ and statefinder pair $\{r, s\}$, $Om(z)$ parameter.

- We first performed MCMC analysis for our $f(Q)$ model to obtain best-fit values of free parameters. To test the fits provided by MCMC, we obtained theoretical predictions for the Hubble parameter $H(z)$, deceleration parameter $q(z)$ and statefinder pair $\{r, s\}$, $Om(z)$ parameter.
- As we noticed, the Hubble parameter respected low redshift observations, and the deceleration parameter provided correct values of q_0 and transitional redshift within the constrained range. Moreover, statefinder diagnostics predict that the Universe was initially in the Quintessence phase, passing the Λ CDM state and returning to Quintessence again.
- We plotted non-linear matter power spectra (with/without RSDs) for both small and large simulation volumes, respectively, where we plotted CAMB linear/non-linear power spectra and observational data from Ly- α forest for the sake of comparison.
- One can notice that within the permitted range of wavenumber k , non-linear matter power spectra from small/large N-body simulations coincide with the CAMB one. However, for $L_{\text{Box}} = 10h^{-1}\text{Mpc}$, non-linear P_k coincide with linear CAMB prediction too early because of the small box size.
- One can check the newly upcoming observational data to investigate the other cosmological scenarios and tensions in these modified theories of gravity.

Thank you for your attention!